ELSEVIER

Biochimica et Biophysica Acta 1514 (2001) 239–252

BIOCHIMICA ET BIOPHYSICA ACTA
BBA

www.bba-direct.com

Lipopolysaccharide can activate BK channels of arterial smooth muscle in the absence of iNOS expression

Natalia Yakubovich, Jodene Renee Eldstrom, David Alexander Mathers *

Department of Physiology, University of British Columbia, 2146 Health Sciences Mall, Vancouver, BC, Canada V6T 1Z3

Received 23 April 2001; received in revised form 19 June 2001; accepted 21 June 2001

Abstract

The role of inducible nitric oxide synthase (iNOS) in the acute activation of large-conductance, Ca^{2+}-dependent K^+ channels (BK channels) by *Escherichia coli* endotoxin (lipopolysaccharide, LPS) was studied in murine vascular smooth muscle cells. Confocal laser scanning microscopy and patch clamp recordings were utilised. Within 2 h of donor rat sacrifice, iNOS-like immunoreactivity could be detected in cerebrovascular smooth muscle cells (CVSMCs) enzymatically dispersed from rat cerebral arteries. This staining was absent in cells fixed immediately after donor rat sacrifice. LPS was then applied to the cytoplasmic face of inside-out membrane patches excised from rat CVSMCs within 2–4 h of donor rat sacrifice. It was found that LPS (10–100 μg/ml) rapidly and reversibly increased the open probability of BK channels in these patches. This LPS response was not altered in the presence of the non-isoform specific NOS inhibitor N^{ω}-nitro-L-arginine. LPS responses were then compared in aortic smooth muscle (ASMC) BK channels derived from wild-type and iNOS-knockout (iNOS-KO) mice. LPS activated BK channels in inside-out patches of ASMC membrane derived from both wild-type and iNOS-knockout mice. These studies establish that LPS can activate BK channels by a mechanism quite independent of the well-established pathway mediated by iNOS in vascular smooth muscle cells.

Keywords: Vascular smooth muscle cell; Ca^{2+}-activated potassium channel; BK channel; Lipopolysaccharide; Inducible nitric oxide synthase; iNOS knockout mouse

1. Introduction

Inducible nitric oxide synthase (iNOS) [1,2] is expressed in vascular smooth cells (VSMCs) following exposure to a variety of stimuli, including bacterial endotoxin (lipopolysaccharide, LPS) [3–5], ageing [6], hypertension [7], traumatic brain injury [8], pro-inflammatory cytokines [9], anoxia [10] and ischaemia [11,12].

Following iNOS induction, the L-arginine-nitric oxide-guanosine-3′,5′-cyclic monophosphate-dependent protein kinase (L-Arg-NO-PKG) pathway of VSMCs is activated. NO synthesised from L-Arg by iNOS activates soluble guanylate cyclase (sGC), leading to cGMP formation and activation of PKG [13,14]. In turn, PKG phosphorylates a number of target proteins, including large conductance, Ca^{2+}-dependent K^+ channels (BK channels) in VSMCs [15–17]. Phosphorylation by PKG results in excessive activation of BK channels, hyperpolarisation of the VSMC membrane and abnormal dilation of systemic and cerebral vessels [18,19]. These changes are believed to contribute to the pathophysiology of both septic shock and bacterial meningitis [4,20,21].

* Corresponding author. Fax: +1-604-822-6048.
E-mail address: mathers@interchange.ubc.ca (D.A. Mathers).

0005-2736/01/$ – see front matter
PII: S0005-2736(01)00378-9

The important role of iNOS in mediating vascular changes evoked by LPS has been verified in mice deficient for the gene encoding this enzyme [22]. Carotid artery preparations from iNOS-knockout (iNOS-KO) mice do not develop the LPS-induced hyporesponsiveness to constrictor agents typically seen in vessels from wild-type mice [23]. In addition, LPS produces less hypotension in iNOS-KO mice [24,25].

Previously, we reported a novel action of LPS on the BK channels found in rat cerebrovascular smooth muscle cells (CVSMCs) [26,27]. These studies employed enzymatically dispersed CVSMCs maintained in vitro at 4°C for 2 days prior to use. It was found that acute application of 100 μg/ml *Escherichia coli* LPS to the cytoplasmic face of inside-out patches of CVSMC membrane rapidly increased the open probability of BK channels by about threefold over control values [26]. When CVSMCs were preincubated for 20 min in the presence of the non-isoform specific NOS inhibitor N^{ω}-nitro-L-arginine (L-NNA, 50 μM), LPS application no longer altered the open probability of BK channels. D-NNA, which is much less active than L-NNA as a NOS antagonist, did not prevent BK channel activation by LPS. However, incubation in the presence of the NOS substrate L-arginine (L-Arg, 1 μM) doubled the increase in P_o seen on application of LPS [27].

Accordingly, it was suggested that NOS activation might play a role in the acute stimulation of BK channels by LPS [27]. Since iNOS is generally believed to be the major NOS isoform expressed in VSMCS [6,28], the acute activation of BK channels by LPS might require prior induction of iNOS in vascular smooth muscle cells.

If iNOS activity is indeed essential for the acute activation of BK channels by LPS, this response should be absent in VSMCs derived from iNOS-KO mice. Furthermore, BK channel activation by LPS should always be suppressed by NOS inhibitors, regardless of the protocol used for cell isolation. We have now tested these predictions using freshly isolated rat CVSMCs, studied within 2–4 h of donor rat sacrifice, and aortic smooth muscle cells (ASMCs) derived from both normal and iNOS-KO mice.

Although cloned mouse BK channels have been thoroughly studied [29,30], native BK channels in mouse vascular tissues have received relatively little attention [31]. Accordingly, we also investigated the biophysical properties of BK channels found in mouse ASMCs.

2. Materials and methods

CVSMCs were enzymatically dissociated from the cerebral arteries of adult Wistar rats (250–300 g). Arteries were incubated for 30 min at 37°C in 0.06% protease (Type XXIV, Sigma, St. Louis, MO), 0.05% collagenase (Type 1A, Sigma) and 0.04% trypsin inhibitor (Type II-S, Sigma). Enzymes were applied in Ca^{2+}-free Tyrode's solution of composition (mM): NaCl 138, KCl 4.5, $MgCl_2$ 0.5, Na_2HPO_4 0.33, HEPES 10, glucose 5.5; pH 7.4. Cells were then washed and dispersed by trituration in a holding solution of composition (mM): KOH 70, KCl 70, L-glutamate 50, taurine 20, $MgCl_2$ 0.5, K_2HPO_4 1 EGTA 0.5, HEPES 10, creatine 5, pyruvate 5 and Na_2ATP 5; pH 7.4. Cells were then plated onto glass coverslips and maintained at 4°C in holding solution. Cells were used for recordings within 4 h of donor rat sacrifice.

ASMCs were dispersed from the thoracic aortas of wild-type CD1 white mice (4–6 weeks old) and from homozygous C57BL/6-*Nos2*^{tm1Lau} (iNOS-KO) mice (6 weeks old, The Jackson Laboratory, Bar Harbor, ME). Aortas were first washed in Ca^{2+}-free Tyrode's solution, cut into pieces, and incubated for 40 min at 37°C in this solution supplemented with 0.06% protease (Type XXIV, Sigma), 0.06% elastase (Type IIA, Sigma), 0.05% collagenase (Type 1A, Sigma) and 0.04% trypsin inhibitor (Type IIS, Sigma). Aortic fragments were washed and triturated in 1 ml of holding solution, of composition described previously. Cells were plated onto glass coverslips and maintained at 4°C in holding solution until use within 4 h of donor mouse sacrifice.

Patch clamp recordings were obtained at 21–23°C. Standard methods were used to isolate inside-out membrane patches from relaxed CVSMCs and ASMCs [32]. Patch electrodes were filled with solution A of composition (mM): KCl 140, $CaCl_2$ 1.48, HEPES 10, EGTA 3; pH 7.4 (free calcium concentration 50 nM). The cytoplasmic face of inside-out membrane patches was typically bathed in solution B of composition (mM): KCl 140, $CaCl_2$ 2.78, HEPES

10, EGTA 3; pH 7.4 (free internal calcium concentration 0.65 μM). LPS (*E. coli* serotype 0127:B8) and N^{ω}-nitro-L-arginine (L-NNA) were obtained from Sigma and dissolved in solution B prior to application to the cytoplasmic face of isolated inside-out membrane patches. In experiments involving L-NNA, cells were pre-incubated in 100 μM L-NNA for at least 15 min at 21°C, prior to patch excision.

Single BK channel currents were recorded on videotape with a bandwidth of DC-2 kHz and analysed using commercial software. Exponential terms were fitted to the observed open and closed time distributions. Current amplitude distributions were fitted by Gaussian functions. The open probability, P_o of single BK channels was calculated from the relation $P_o = (T_1 + 2T_2 + \ldots NT_N)/NT_{tot}$, where N was the number of BK channels in the patch, T_{tot} the total record duration, and T_1, $T_2 \ldots T_N$ the times when at least 1,2...N channels were open. BK channels were identified by their large conductance (>190 pS in symmetrical 140 mM K^+), block by 25 mM tetraethylammonium (TEA^+) (Sigma) or by 5 nM free calcium saline applied to the cytoplasmic membrane surface [26]. Results were expressed as mean ± S.E.M and analysis of variance (ANOVA) methods were employed to evaluate differences between experimental groups.

To determine the distribution of iNOS-like immunoreactivity in rat CVSMCs, rat brains were removed, fixed immediately in 4% paraformaldehyde, and preserved in phosphate-buffered saline (PBS) containing 20% sucrose. Forty-μm thick cryostat sections showing transverse views through cerebral arteries and were blocked by 30 min incubation at 21°C in PBS containing 10% goat serum, 1% bovine serum albumin and 0.2% Triton X-100. Dispersed rat CVSMCs prepared as noted previously were fixed and blocked in similar fashion.

Tissue sections and dispersed cells were double-labelled by incubation for 48 h at 4°C with the following primary antibodies: monoclonal mouse IgG anti-smooth muscle α-actin (1:7000, Sigma) and polyclonal rabbit anti-iNOS (1:100, BD Transduction Laboratories, Mississauga, ON). Preparations were then washed in PBS and incubated for 90 min at room temperature with the following secondary antibodies: goat anti-mouse IgG, Alexa-594 labelled (1:7000, Molecular Probes, Eugene, OR) and goat anti-rabbit IgG, Alexa-488 labelled (1:2000, Molecular Probes). Labelled cells were viewed under a Zeiss Axiophot indirect immunofluorescence microscope, or examined by confocal laser scanning microscopy (CLSM) using a Biorad MRC 600 equipped with NIH Image and Photoshop digital image analysis software.

3. Results

The expression of iNOS in rat CVSMCs was investigated using immunocytochemical methods applied to brains fixed immediately after donor rat sacrifice. Fig. 1 shows a transverse section through the middle cerebral artery, co-labelled with fluorescent probes for smooth muscle α-actin and iNOS immunoreactivity. As expected, extensive α-actin-like immunoreactivity was detected throughout the vessel media (Fig. 1A). In contrast, iNOS-like immunoreactivity was essentially absent from the same tissue section (Fig. 1B).

We next investigated the occurrence of iNOS-like immunoreactivity in CVSMCs which had been enzymatically dispersed from rat cerebral arteries. Fig. 2A shows smooth muscle α-actin-like immunoreactivity detected in a CVSMC fixed a total of 2 h after donor sacrifice. Staining was present mainly under the sarcolemma in these cells. Fig. 2B illustrates the pattern of iNOS-like immunoreactivity in the same cell. Extensive cytoplasmic labelling was detected in most CVSMCs examined, with the central, nuclear regions of these cells remaining unstained. Fig. 2C shows the result of overlaying staining patterns for both immunoprobes in this cell. The occurrence of yellow/orange staining in the periphery indicated that iNOS-like immunoreactivity was present in the actin-rich region under the sarcolemma. This pattern of staining was seen in the majority of CVSMCs examined. These results indicated that iNOS-like immunoreactivity is rapidly induced in rat CVSMCs upon enzymatic dispersion of these cells from intact arteries.

As a functional test for iNOS involvement in the acute response of BK channels to LPS, we next compared these responses in the absence and presence of L-NNA. This competitive NOS antagonist inhibits

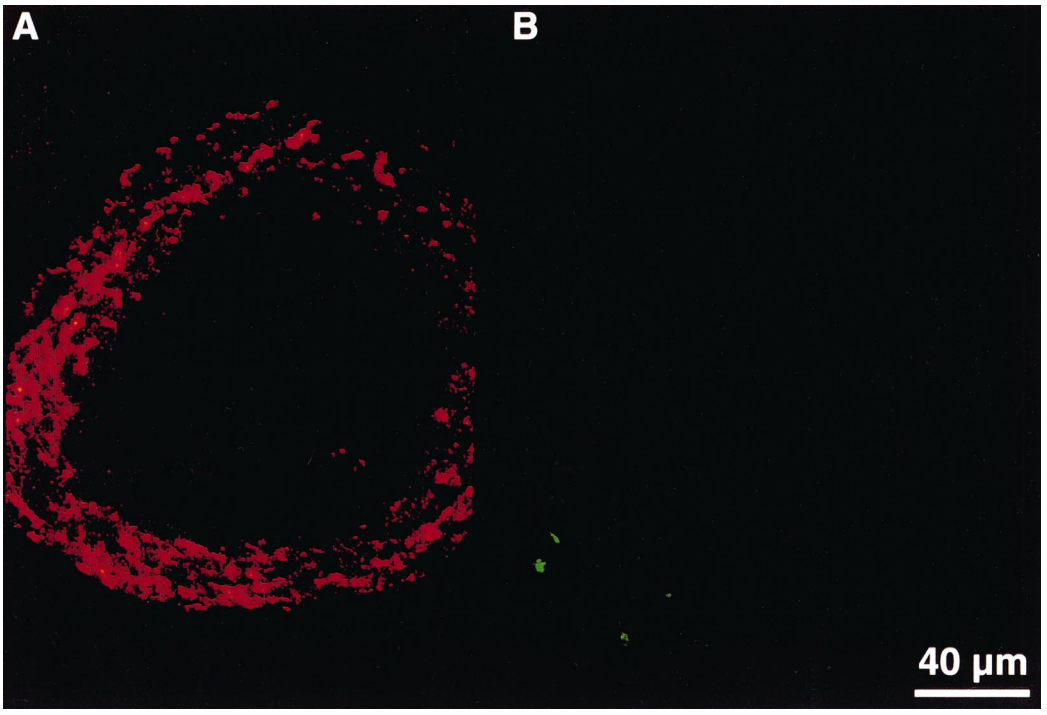

Fig. 1. Smooth muscle α-actin-like immunoreactivity, visualised with a red fluorophore and iNOS-like immunoreactivity (green fluorophore) in the same transverse section of rat middle cerebral artery, fixed immediately on donor rat sacrifice. (A) Extensive labelling for smooth muscle α-actin-like immunoreactivity was seen in the vessel media. (B) iNOS-like immunoreactivity was essentially absent. Sections were visualised by CLSM methods.

the iNOS expressed in rat vascular smooth muscle cells with an IC_{50} in the range of 1–10 μM [33]. These recordings employed inside-out patches excised from CVSMCs within 2–4 h of donor rat sacrifice.

Fig. 3A shows the effect of acutely applying 50 μg/ml LPS to the cytoplasmic face of an inside-out patch of CVSMC membrane, voltage-clamped to a membrane potential, $V_m = -30$ mV. Within 30 s, LPS markedly increased the open probability of the single BK channel in this membrane patch. This effect rapidly reversed upon wash-out of endotoxin.

In Fig. 3B, this experiment was repeated employing dispersed CVSMCs which had been pre-incubated for 30 min in 100 μM L-NNA prior to membrane patch excision. This concentration of L-NNA

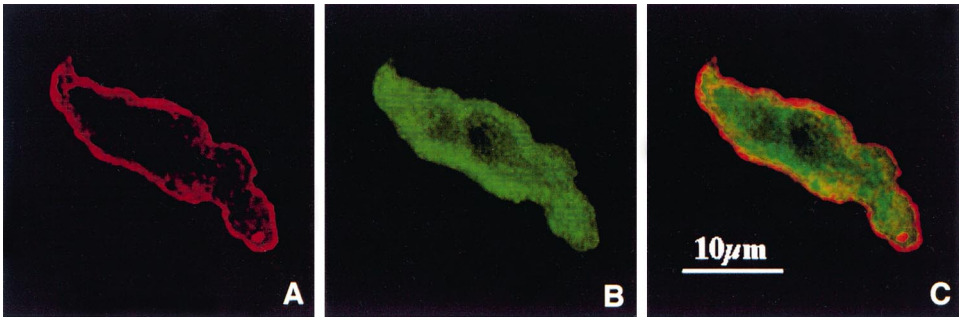

Fig. 2. Smooth muscle α-actin-like and iNOS-like immunoreactivities in the same rat CVSMC fixed 2 h after donor rat sacrifice. (A) Smooth muscle α-actin-like immunoreactivity, visualised with a red fluorophore, was present under the sarcolemma. (B) iNOS-like immunoreactivity (green fluorophore) was seen throughout the cytoplasm, with sparing of the central nuclear region. (C) Overlay of images seen in A and B. Yellow/orange staining indicated co-localisation of both types of immunoreactivities in this cell. Images were obtained using CLSM methods.

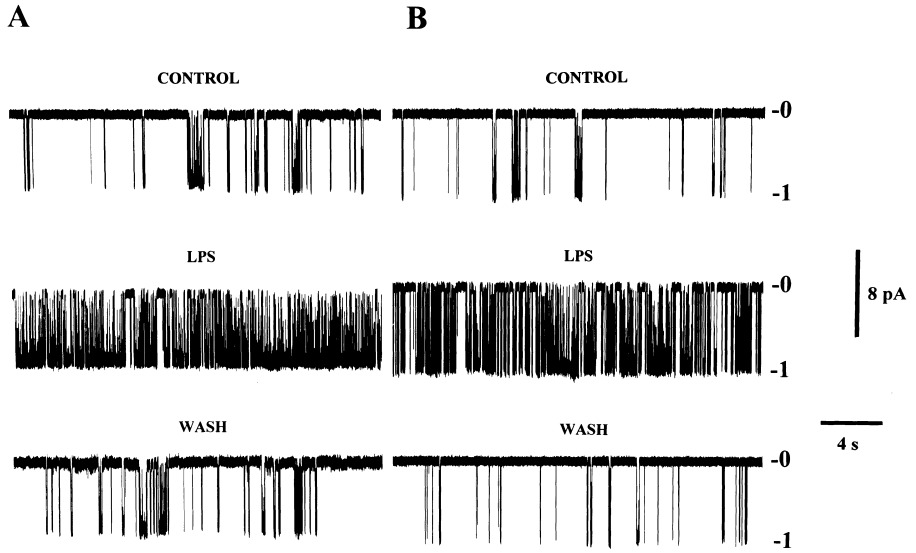

Fig. 3. Effect of LPS on single BK channels present in isolated, inside-out membrane patches excised from rat CVSMCs within 3 h of donor rat sacrifice. LPS (50 μg/ml) was applied to the cytoplasmic membrane face and both patches were voltage-clamped to $V_m = -30$ mV with $[Ca^{2+}]_i = 0.65$ μM. (A) Rapid, reversible activation of a single BK channel in a membrane patch studied in the absence of the NOS inhibitor L-NNA. (B) A second membrane patch studied in the presence of 100 μM L-NNA at the cytoplasmic membrane face. Application of LPS to this patch also activated the single BK channel it contained. Numbers at right of these recordings indicate patch current levels when BK channels are closed (0) or open (1). Bandwidth of recordings DC-2 kHz.

was also present in all solutions applied to the cytoplasmic face of excised patches. It can be seen that application of 50 μg/ml LPS to the cytoplasmic face of this test patch again resulted in rapid and reversible activation of the single BK channel present.

The results obtained from a number of experiments of this type are summarised in Fig. 4. It can be seen that LPS significantly increased the open probability of single BK channels and that the magnitude of this potentiation was unaffected by the presence of L-NNA. Similarly, L-NNA did not alter the open probability of BK channels measured in the absence of LPS.

These data were further analysed to determine the effects of LPS on the conductance and kinetic properties of single BK channels. LPS (50 μg/ml) had no significant effects on the conductance of BK channels (Control, 235 ± 23 pS; LPS, 239 ± 21 pS, $n = 6$ patches, $P > 0.05$, ANOVA). When measured in the presence of 100 μM L-NNA, again no change in conductance was seen on application of LPS (L-NNA alone, 251 ± 23 pS; L-NNA+LPS, 249 ± 22 pS, $n = 4$, $P > 0.05$, ANOVA).

The effect of LPS on the distribution of open times of single BK channels is shown in Fig. 5A. In both the absence and presence of LPS, open time distributions were well described by the sum of two exponential terms, that is $y = A_{of}e^{-t/\tau_{of}} + A_{os}e^{-t/\tau_{os}}$. Here, the fast and slow time constants τ_{of} and τ_{os} governed the amplitude terms A_{of} and A_{os}, respectively. Measurement of these parameters allowed cal-

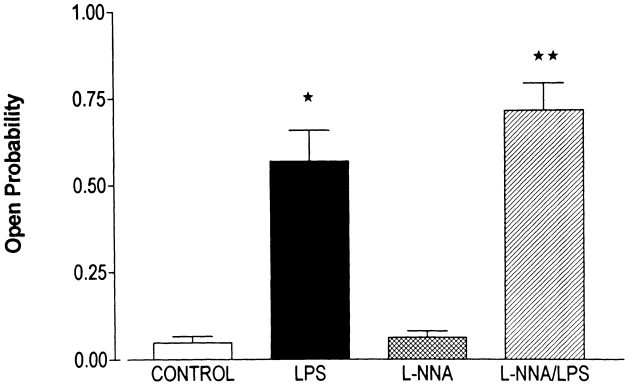

Fig. 4. Effect of 50 μg/ml LPS on the open probability of BK channels studied in inside-out patches of rat CVSMC membrane. $n = 8$ patches were studied in the absence of L-NNA, data being obtained before (Control) and during application of LPS (LPS). A further $n = 6$ patches were studied in the continuous presence of 100 μM L-NNA, data being obtained before (L-NNA) and during LPS application (L-NNA/LPS). *Significantly different from the Control value. **Significantly different from the L-NNA value ($P < 0.05$, ANOVA), but not significantly different from the LPS value. All data were obtained at $V_m = -30$ mV with $[Ca^{2+}]_i = 0.65$ μM.

culation of the mean open time of BK channels, using the relation $\tau_{\text{mean open}} = A_{\text{of}}/(A_{\text{of}}+A_{\text{os}})\tau_{\text{of}}+A_{\text{os}}/(A_{\text{of}}+A_{\text{os}})\tau_{\text{os}}$. As shown in Table 1, LPS had no significant effect on the values of τ_{of}, τ_{os} and of $\tau_{\text{mean open}}$). L-NNA (100 μM) itself had no effect on the values of these parameters (Table 1). When measured in the presence of 100 μM L-NNA, again no changes were seen in the values of τ_{of}, τ_{os} and $\tau_{\text{mean open}}$ upon the application of 50 μg/ml LPS (Table 1). These observations indicate that neither LPS nor L-NNA significantly alters the conductance or the average lifetime of BK channels in the open state.

The effect of LPS on the distribution of closed times for single BK channel currents is shown in Fig. 5B. In both the absence and presence of 50 μg/ml LPS, closed time distributions were well described by the sum of three exponential terms, that is $y = A_{\text{cf}}e^{-t/\tau_{\text{cf}}} + A_{\text{cm}}e^{-t/\tau_{\text{cm}}} + A_{\text{cs}}e^{-t/\tau_{\text{cs}}}$. Measurement of these parameters allowed calculation of the mean channel closed time as $\tau_{\text{mean close}} = A_{\text{cf}}/(A_{\text{cf}}+A_{\text{cm}}+A_{\text{cs}})\tau_{\text{cf}}+A_{\text{cm}}/(A_{\text{cf}}+A_{\text{cm}}+A_{\text{cs}})\tau_{\text{cm}}+A_{\text{cs}}/(A_{\text{cf}}+A_{\text{cm}}+A_{\text{cs}})\tau_{\text{cs}}$. As shown in Table 1, LPS had no effect on the value of τ_{cf} or τ_{cm}. However, the time constant governing long duration closures, τ_{cs} was significantly reduced in the presence of LPS, as was the value of $\tau_{\text{mean close}}$ (Table 1).

L-NNA (100 μM) had no effects on τ_{cf}, τ_{cm}, τ_{cs} or $\tau_{\text{mean close}}$ and did not significantly alter the effects of LPS on the latter two parameters (Table 1). These observations indicated that LPS increased BK channel open probability by accelerating the rate of reopening from long-duration channel closures. This mechanism was completely unaltered in the presence of the nitric oxide synthase inhibitor L-NNA.

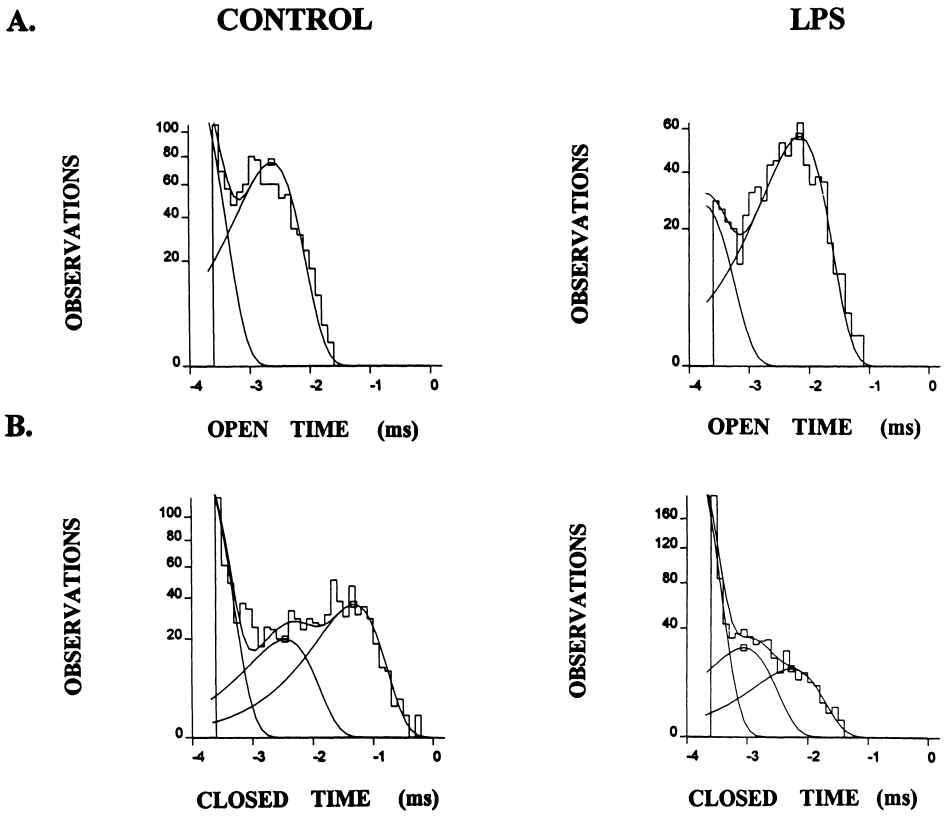

Fig. 5. Effects of 50 μg/ml LPS on the kinetics of a single BK channel in an inside-out patch of rat CVSMC membrane, voltage-clamped to $V_m = -30$ mV with $[Ca^{2+}]_i = 0.65$ μM. (A) Open time distributions obtained in Control (954 channel openings) and LPS-containing salines (724 openings). Each distribution was well described by the sum of two exponential terms (smooth curves) using the following fit parameters, defined in the text. Control: $\tau_{\text{of}} = 0.12$ ms; $\tau_{\text{os}} = 2.4$ ms. LPS: $\tau_{\text{of}} = 0.16$ ms; $\tau_{\text{os}} = 6.8$ ms. (B) Corresponding closed time distributions from the same recordings used in A. These distributions were well-described by the sum of three exponential terms (smooth curves) using the following parameters. Control (961 closings): $\tau_{\text{cf}} = 0.14$ ms; $\tau_{\text{cm}} = 3.5$ ms; $\tau_{\text{cs}} = 47.8$ ms. LPS (686 closings): $\tau_{\text{cf}} = 0.10$ ms; $\tau_{\text{cm}} = 0.90$ ms; $\tau_{\text{cs}} = 5.4$ ms.

Table 1
Effects of 50 μg/ml LPS on the gating kinetics of BK channels studied in inside-out patches of rat CVSMC membrane

Parameter (ms)	Control	LPS	L-NNA	L-NNA+LPS
τ_{of}	0.7 ± 0.1	1.0 ± 0.2	0.9 ± 0.1	1.6 ± 0.5
τ_{os}	9 ± 2.3	14 ± 4.0	12 ± 2.5	18 ± 3.3
$\tau_{mean\ open}$	7 ± 2.1	12 ± 3.4	10 ± 2.6	14 ± 3.5
τ_{cf}	0.7 ± 0.2	0.3 ± 0.1	0.5 ± 0.1	0.5 ± 0.2
τ_{cm}	23 ± 6.8	6 ± 2.9	19 ± 9.0	3 ± 0.7
τ_{cs}	350 ± 54	64 ± 27*	423 ± 72	31 ± 7**
$\tau_{mean\ close}$	119 ± 40	7.2 ± 2.9*	110 ± 21	4.1 ± 2.3**

Patches were voltage-clamped to $V_m = -30$ mV with $[Ca^{2+}]_i = 0.65$ μM. See text for explanation of symbols used. The table shows kinetic parameters obtained from $n = 7$ patches untreated with L-NNA (Control vs. LPS) and $n = 6$ patches studied in the presence of 100 μM L-NNA (L-NNA vs. L-NNA+LPS). Values given are mean ± S.E.M. *Significantly different from the corresponding Control value obtained in absence of LPS ($P < 0.05$, ANOVA). **Significantly different from the value obtained in the presence of L-NNA only, but not significantly different from the value obtained with LPS only.

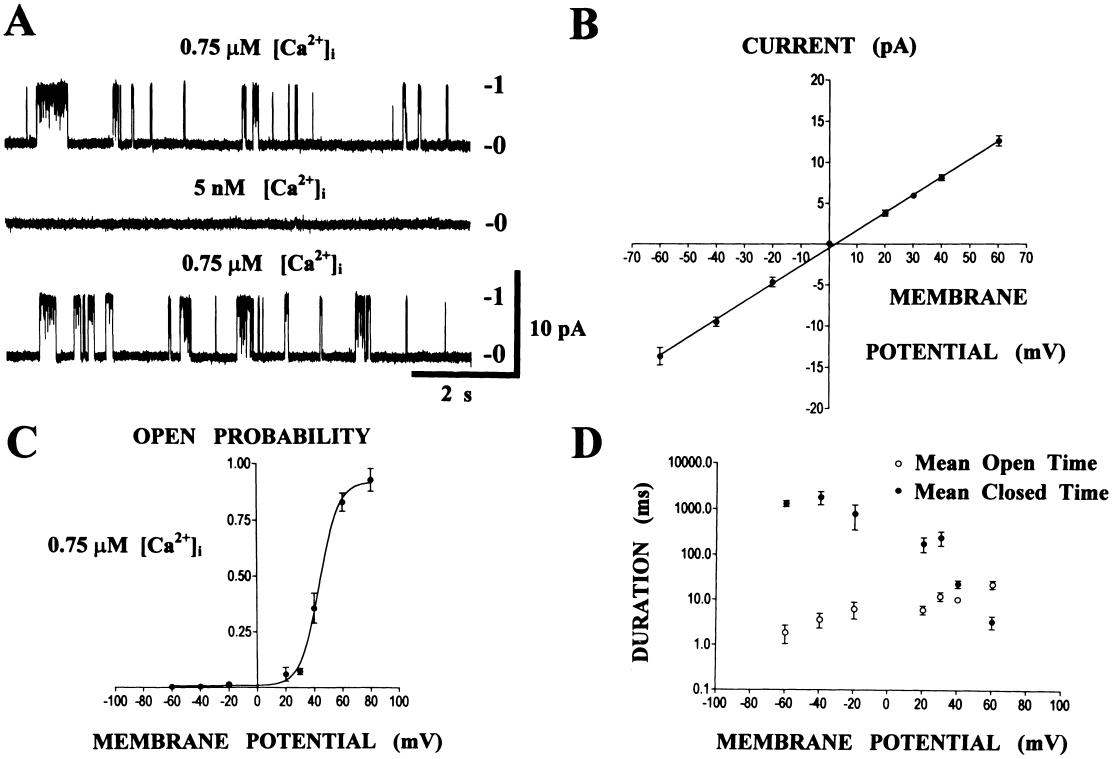

Fig. 6. Biophysical characterisation of single BK channel currents studied in inside-out membrane patches excised from ASMCs of wild-type mice. (A) Reversible abolition of BK channel currents on reducing the concentration of free Ca^{2+} bathing the cytoplasmic membrane face from $[Ca^{2+}]_i = 0.75$ μM to $[Ca^{2+}]_i = 5$ nM. This patch was voltage-clamped to $V_m = +30$ mV. Channel closed and channel open current levels are indicated by 0 and 1, respectively. (B) Current–voltage relation of single BK channels exposed to symmetrical 140 mM K^+ salines on both membrane faces. Data were obtained from $n = 11$ patches. The straight line fitted by linear regression had a slope of 218 pS and a reversal potential of +2.3 mV. (C) Activation curve for single BK channel currents, obtained in the presence of $[Ca^{2+}]_i = 0.75$ μM. Data were derived from $n = 11$ patches. The smooth curve is the best-fit Boltzmann relation, drawn to the equation $P_o = 1/(1 + e^{-K(V_m - V_o)})$ with $K = 0.15$ mV^{-1} and $V_o = +43.8$ mV. (D) Effect of membrane potential on the mean open time (○) and mean closed time (●) of single BK channels. Data were obtained from $n = 8$ patches studied at $[Ca^{2+}]_i = 0.75$ μM.

To further study the putative role of iNOS in the acute response of BK channels to LPS, a second series of experiments was carried out on freshly dispersed ASMCs obtained from wild-type and iNOS-KO mice. The biophysical properties of these channels were firstly characterised in inside-out membrane patches excised from wild-type ASMCs within 2–4 h of donor mouse sacrifice.

Single BK channel currents detected in an inside-out membrane patch voltage-clamped to $V_m = +30$ mV are seen in Fig. 6. These currents were reversibly suppressed by reducing the concentration of free Ca^{2+} perfusing the cytoplasmic membrane face from $[Ca^{2+}]_i = 0.75$ μM to 5 nM (Fig. 6A). The single channel current-voltage relation for mouse BK channels is shown in Fig. 6B. This plot yielded an average slope conductance of 218 ± 5 pS ($n = 11$ patches) and a reversal potential of +2.3 mV in symmetrical 140 mM K^+, very close to the expected value of 0 mV.

Mouse BK channels exhibited strongly voltage-dependent gating when examined in the presence of solutions containing $[Ca^{2+}]_i = 0.75$ μM. Fig. 6C shows the single channel activation curve obtained by averaging data from $n = 11$ patches. These data were well fit by the smooth curve drawn to the Boltzmann relation $P_o = \{1+\exp[-K(V_m - V_o)]\}^{-1}$. Here K was a slope factor describing the steepness of voltage dependence and V_o was the membrane potential at which $P_o = 0.5$. The best fit was obtained using $K = 0.15$ mV^{-1} and $V_o = +44$ mV. Fig. 6D indicates that depolarisation raised the open probability of mouse BK channels both by reducing the mean channel closed time, and by increasing the mean duration of these channels in the open state.

Fig. 7 demonstrates that mouse BK channels were

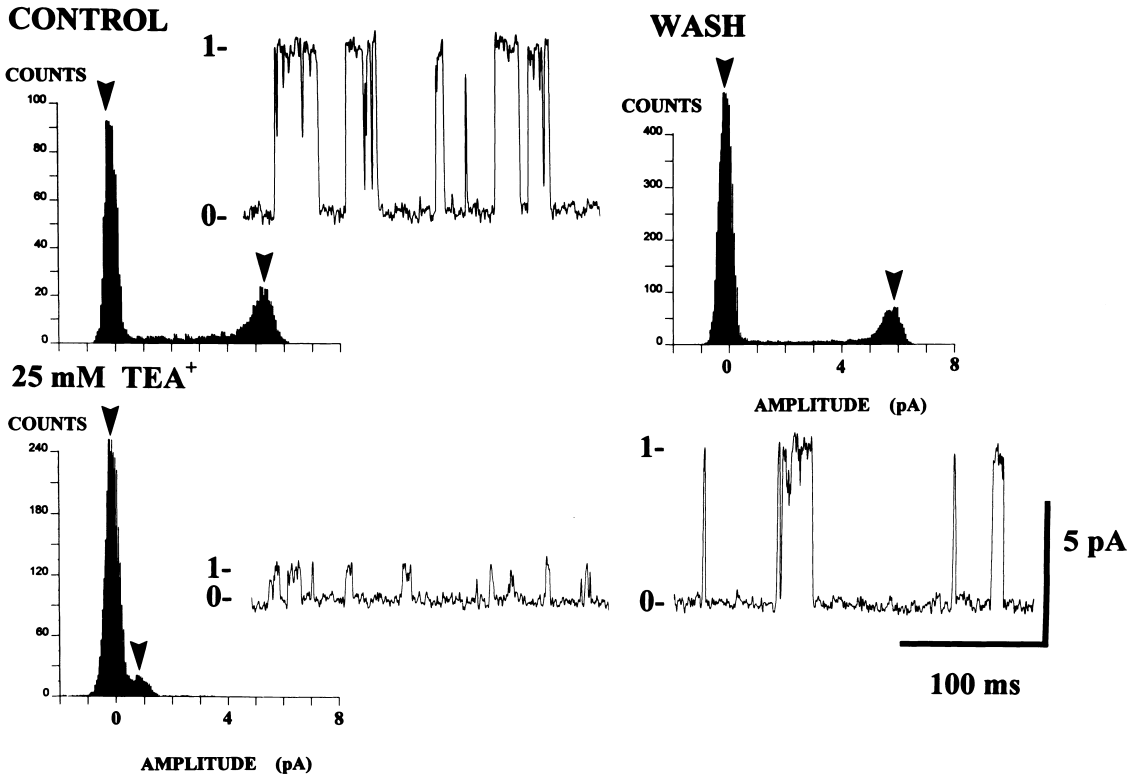

Fig. 7. Effect of TEA^+ on single BK channel currents recorded from an inside-out patch of ASMC membrane obtained from a wild-type mouse. This patch contained one active BK channel. The figure shows all-points histograms of patch current obtained before (Control), during (25 mM TEA^+), and after application of TEA^+ to the cytoplasmic membrane face (Wash). Each histogram contains two peaks (arrows), corresponding to mean current amplitude when the channel is closed (~0 pA) and when it is open. Note that TEA^+ application markedly reduced mean current in the open state. Each histogram is accompanied by a representative trace from the data which generated it. In these traces, 0 denotes closed channel current while 1 denotes current in the open state. All data were obtained at $V_m = +30$ mV with $[Ca^{2+}]_i = 0.75$ μM.

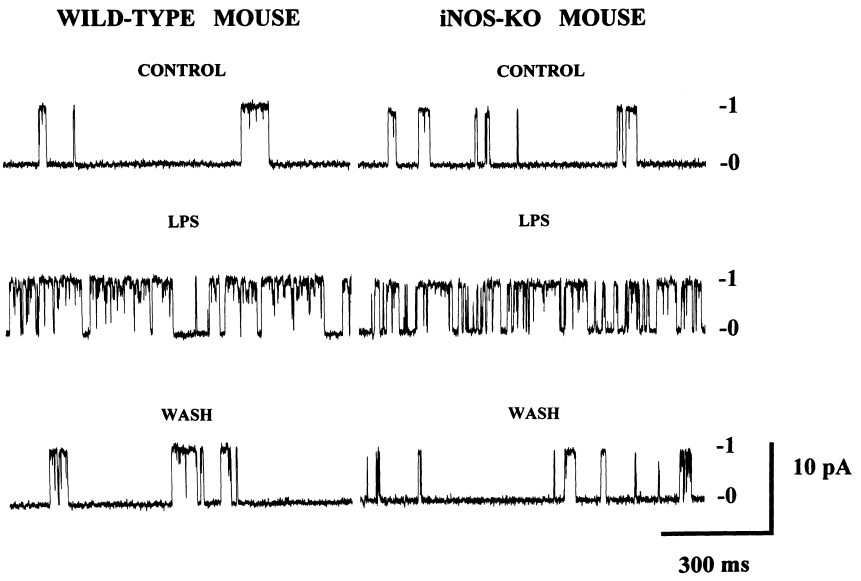

Fig. 8. Effects of LPS on BK channels present in inside-out membrane patches of ASMC membrane derived from wild-type and iNOS-KO mice. LPS (50 μg/ml) was applied to the cytoplasmic membrane face and both patches were voltage-clamped to $V_m = +30$ mV with $[Ca^{2+}]_i = 0.75$ μM. Left-hand panels: rapid, reversible activation of a single BK channel in an ASMC membrane patch derived from a wild-type mouse. Right-hand panels: data from an ASMC membrane patch derived from an iNOS-KO mouse. Application of LPS to this patch also activated the single BK channel it contained. Numbers at right of these recordings indicate patch current levels when BK channels are closed (0) or open (1). Bandwidth of recordings DC-2 kHz.

susceptible to block by application of TEA^+ to the cytoplasmic face of inside-out membrane patches. Application of 25 mM TEA^+ to 5 patches voltage-clamped at $V_m = +30$ mV resulted in a mean reduction in single channel current to $37 \pm 7\%$ of the control value. Similar biophysical properties have been reported for single BK channels in vascular myocytes of the rat [32,34] and of the rabbit [35,36].

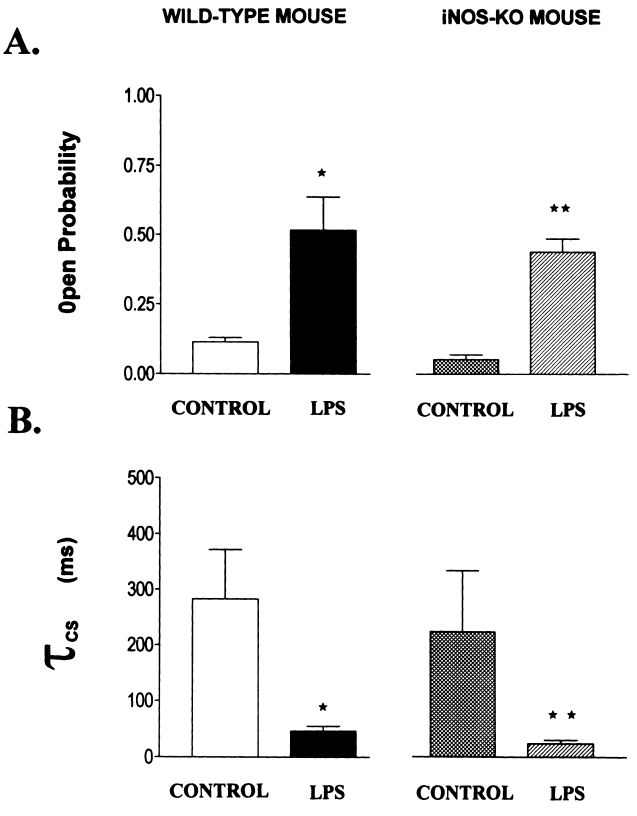

Fig. 9. Effect of 100 μg/ml LPS on the open probability and gating of BK channels studied in inside-out patches of ASMC membrane derived from wild-type and iNOS-KO mice. (A) Open probabilities obtained before (Control) and during application of LPS (LPS) in patches derived from wild-type (left-hand panel, $n = 6$) and iNOS-KO mice (right-hand panel, $n = 5$). *Significantly different from the corresponding Control value. **Significantly different from the corresponding Control value ($P < 0.05$, ANOVA), but not significantly different from the LPS value seen in wild-type mice. (B) Time constant of long-duration channel closures, τ_{cs} obtained before (Control) and during LPS application (LPS) in patches derived from wild-type (left-hand panel, $n = 5$) and iNOS-KO mice ($n = 5$). *Significantly different from the corresponding Control value. **Significantly different from the corresponding Control value ($P < 0.05$, ANOVA), but not significantly different from the LPS value seen in wild-type mice. All data were obtained at $V_m = +30$ mV with $[Ca^{2+}]_i = 0.75$ μM.

Fig. 8 compares the LPS responses of BK channels derived from the ASMCs of wild-type and iNOS-KO mice. These inside-out membrane patches were voltage-clamped to $V_m = +30$ mV and 50 μg/ml LPS was applied to the cytoplasmic membrane face. LPS significantly increased the open probability of BK channels derived from both mouse strains. Moreover, the degree of potentiation seen in P_o did not differ between the two mouse strains (Fig. 9A). LPS had no effect on the conductance of BK channels from either wild-type (Control, 207 ± 14 pS; LPS, 202 ± 14 pS, $n = 6$, $P > 0.04$, ANOVA) or iNOS-KO strains (Control, 202 ± 19 pS; LPS, 197 ± 19 pS, $n = 5$, $P > 0.05$, ANOVA). Control values of conductance also did not differ between the two mouse strains.

Kinetic analysis was performed to determine the effects of LPS on gating parameters. As found previously for rat channels, BK channels derived from wild-type mice displayed open time distributions which were well described by the sum of two exponential terms (Fig. 10A). Closed time distributions required the sum of three exponentials (Fig. 10B). Again as found in the rat, application of LPS altered only the time constant governing long-duration channel closures, τ_{cs}, decreasing the value of this parameter, and hence lowering the value of $\tau_{mean\ close}$ (Table 2 and Fig. 9B).

The gating behaviour of BK channels derived from iNOS-KO mice was qualitatively and quantitatively similar to that seen in channels obtained from wild-type mice (Table 2). Application of LPS to these channels again reduced the value of τ_{cs}, lowering $\tau_{mean\ close}$ but leaving all other kinetic parameters unchanged (Table 2 and Fig. 9B). Therefore the effect

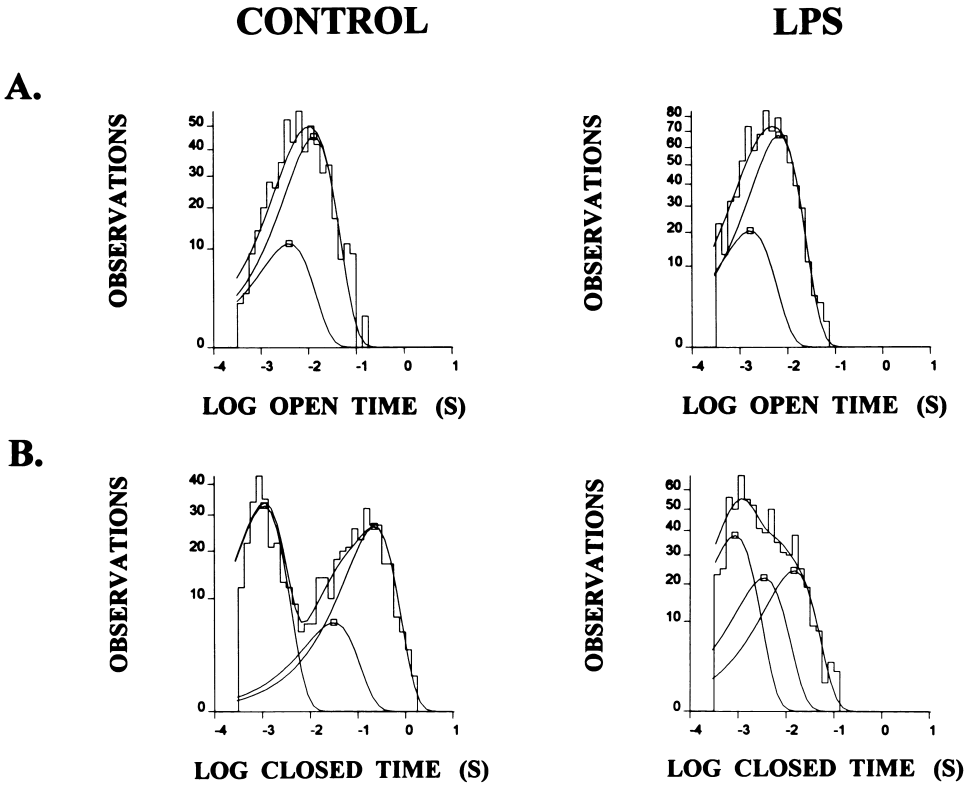

Fig. 10. Effects of 50 μg/ml LPS on the kinetics of BK channels in an inside-out patch of ASMC membrane, derived from a wild-type mouse. This patch was voltage-clamped to $V_m = +30$ mV with $[Ca^{2+}]_i = 0.75$ μM. (A) Open time distributions obtained in Control (532 channel openings) and LPS-containing salines (791 openings). Each distribution was well-described by the sum of two exponential terms (smooth curves) using the following fit parameters, defined in the text. Control: $\tau_{of} = 3.9$ ms; $\tau_{os} = 13.2$ ms. LPS: $\tau_{of} = 1.7$ ms; $\tau_{os} = 6.7$ ms. (B) Corresponding closed time distributions from the same recordings used in A. These distributions were well-described by the sum of three exponential terms (smooth curves) using the following parameters. Control (522 closings): $\tau_{cf} = 1.1$ ms; $\tau_{cm} = 31.2$ ms; $\tau_{cs} = 223$ ms. LPS (660 closings): $\tau_{cf} = 0.9$ ms; $\tau_{cm} = 3.4$ ms; $\tau_{cs} = 14.5$ ms.

Table 2
Effects of 50 μg/ml LPS on the gating kinetics of BK channels studied in inside-out patches of mouse ASMC membrane

Parameter (ms)	Wild-type mouse		iNOS-KO mouse	
	Control	LPS	Control	LPS
τ_{of}	1.9 ± 0.4	1.1 ± 0.3	1.0 ± 0.3	1.0 ± 0.3
τ_{os}	15 ± 4.2	12 ± 4.8	7 ± 1.4	10 ± 1.2
$\tau_{mean\ open}$	12 ± 4.0	10 ± 4.3	6 ± 1.6	8 ± 1.2
τ_{cf}	0.8 ± 0.1	0.6 ± 0.2	0.8 ± 0.1	0.5 ± 0.2
τ_{cm}	26 ± 7.4	11 ± 2.4	30 ± 13	7 ± 2.2
τ_{cs}	207 ± 59	46 ± 9*	114 ± 20	31 ± 11**
$\tau_{mean\ close}$	70 ± 15	14 ± 2.9*	91 ± 16	9 ± 2.8**

Patches were voltage-clamped to $V_m = +30$ mV with $[Ca^{2+}]_i = 0.75$ μM. See text for explanation of symbols used. The table shows kinetic parameters obtained from wild-type mice ($n = 5$ patches) and iNOS-KO mice ($n = 5$ patches). Values given are mean ± S.E.M. *Significantly different from corresponding Control value obtained in absence of LPS ($P < 0.05$, ANOVA). **Significantly different from the iNOS-KO Control value, but not significantly different from the LPS value obtained from wild-type mice.

of LPS on BK channel kinetics was quite independent of the expression of iNOS in mouse ASMCs.

4. Discussion

iNOS-like immunoreactivity was not observed in the smooth muscle cells of cerebral arteries fixed within a few minutes of donor rat sacrifice. This is in agreement with previous studies on these blood vessels in healthy young rats [11,12]. However, iNOS-like immunoreactivity was detected in dispersed CVSMCs examined about 2 h after donor sacrifice. Rat CVSMCs also show evidence of iNOS expression within 2 h of enzyme induction by traumatic brain injury [12]. However, the appearance of iNOS mRNA and iNOS protein typically proceeds with a slower time course in the majority of vascular smooth muscle preparations studied to date. Thus a 24-h delay has been reported for detection of iNOS mRNA following traumatic brain injury in mice [8]. Similarly, a 6-h lag exists between the stimulation of rat ASMCs by endotoxin or cytokines and the appearance of iNOS mRNA and enzyme activity in these cells [4].

The nature of the factors responsible for the rapid expression of iNOS in rat CVSMCs remains unclear. The rapid induction of iNOS in isolated rat cerebral arteries is partially inhibited by the LPS-binding antibiotic polymyxin B [37]. Hence the presence of free LPS in the bathing media may play a role in iNOS induction, as previously suggested [38].

Alternatively, the rapid induction of iNOS in rat CVSMCs may be initiated by the stress and hypoxia which accompany removal of blood vessels from the donor rat. Stress activates immediate early genes [39], products of which can bind to the promoter region of the iNOS gene and enhance iNOS expression [4]. In addition, an hypoxia-responsive element is known to exist in the iNOS promoter region [40]. These regulatory features may contribute to the protective effect of iNOS in minimising long-term neurological deficits following brain injury [8].

iNOS exists both as a free cytoplasmic enzyme and in a post-translationally modified form which associates strongly with organellar membranes [41]. In VSMCs, iNOS exists mainly in the latter form and is closely associated with the sarcoplasmic reticulum and cytoplasmic vesicles [42]. In accord with these findings, the present study revealed the presence of iNOS-like immunoreactivity in an actin-rich, sub-sarcolemmal domain in rat CVSMCs. This domain contains the superficial sarcoplasmic reticulum, which in VSMCs is known to approach within 50 nm of the sarcolemma [43].

In marked contrast to earlier results obtained from cells held in vitro at 4°C for 48 h [27], the LPS response of freshly isolated CVSMCs was not blocked in the presence of the non-isoform specific NOS inhibitor, L-NNA. Moreover, LPS was also found to rapidly activate BK channels in patches of ASMC membrane derived from iNOS-KO mice. These new observations show that neither the expression nor the activation of iNOS is a prerequisite for the acute stimulation of BK channels by endotoxin.

Therefore, LPS can activate BK channels by an

iNOS-independent mechanism in vascular smooth muscle cells. At present, the nature of this novel mechanism remains unclear. However, the fact that LPS exerts its effect rapidly when applied to the cytoplasmic membrane surface suggests the possible involvement of cytoplasmic or membrane spanning domains in the BK channel protein itself.

Such domains are known to play important roles in determining the open probability of BK channels. A cytoplasmic region in the S9-S10 domain of the pore-forming α-subunit contributes to the calcium sensitivity of BK channels [31,44]. In addition, the membrane spanning domain S0 of the α-subunit is unique to the BK channel. It is also essential for the enhanced calcium sensitivity seen in the presence of the regulatory β-subunit [45] which is expressed in vascular smooth muscle cells [31]. LPS may therefore serve as a useful probe to study the interactions of BK channel subunits and the roles of specific protein domains in channel function.

It remains unclear why, in rat CVSMCs maintained in vitro for some time, the LPS response can develop sensitivity to block by NOS inhibitors. However, there is growing evidence that some types of VSMC express constitutive as well as inducible forms of NOS. Thus the neuronal isoform of NOS (nNOS) has been detected in peripheral vessels of the hamster [46], in developing lung vessels of the sheep [47], in bovine carotid arteries [48], and in rat aorta [49]. Human VSMCs also express a constitutive isoform of NOS [50].

nNOS and its subtypes readily form plasma membrane-associated complexes with other enzymes, cytoskeletal proteins and ion channels [51]. Assemblies of this type, formed in rat CVSMCs during maintenance in vitro, may give rise to novel binding sites for arginine analogues in this preparation. Alternatively, L-NNA-sensitive LPS responses may involve an NOS-independent membrane protein which binds arginine analogues and which apparently regulates constriction in rat VSMCs [52].

Acknowledgements

This work was supported by a grant to D.A.M. from the Heart and Stroke Foundation of British Columbia and Yukon.

References

[1] N. Sennequier, D.J. Stuehr, Analysis of substrate-induced, catalytic, and structural changes in inducible NO synthase, Biochemistry 35 (1996) 5883–5892.
[2] J. Marin, M.A. Rodriguez-Martinez, Role of nitric oxide in physiological and pathological conditions, Pharmacol. Ther. 75 (1997) 111–134.
[3] C. Thiemermann, Nitric oxide and septic shock, Gen. Pharmacol. 29 (1997) 159–166.
[4] M. Hecker, M. Cattazura, A.H. Wagner, Regulation of inducible nitric oxide synthase gene expression in vascular smooth muscle, Gen. Pharmacol. 32 (1999) 9–16.
[5] B. Muller, A.L. Kleschyov, K. Gyorgy, J.C. Stoclet, Inducible NO synthase activity in blood vessels and heart: new insight into cell origin and consequences, Physiol. Res. 49 (2000) 19–26.
[6] M.R. Cernadas, J. Sanchez de Miguel, M. Garcia-Duran, F. Gonzales-Fernandez, I. Millas, M. Monton, J. Rodrigo, L. Rico, P. Fernandez, T. de Frutos, J.A. Rodriguez-Feo, J. Guerra, C. Caramelo, S. Casado, A. Lopez-Farre, Expression of constitutive and inducible nitric oxide synthases in the vascular wall of young and aging rats, Circ. Res. 83 (1998) 279–286.
[7] T.-C. Chou, M.-H. Yen, C.-Y. Li, Y.-A. Ding, Alterations in nitric oxide synthase expression with aging and hypertension in rats, Hypertension 31 (1998) 643–648.
[8] E.H. Sinz, P.M. Kochanek, C.E. Dixon, R.S.B. Clark, J.A. Carcillo, J.K. Schiding, M. Chen, S.R. Wisniewski, T.M. Carlos, D. Williams, S.T. Dekosky, S.C. Watkins, D.W. Marion, T.R. Billiar, Inducible nitric oxide synthase is an endogenous neuroprotectant after traumatic brain injury in rats and mice, J. Clin. Invest. 104 (1999) 647–656.
[9] Z.Q. Yan, A. Sirsjo, M.L. Bochaton-Piallat, G. Gabbiani, G.K. Hansson, Augmented expression of inducible NO synthase in vascular smooth muscle cells during aging is associated with enhanced NF-kappaB activation, Arterscler. Thromb. Vasc. Biol. 19 (1999) 2854–2862.
[10] T.D. Le Cras, C. Xue, A. Rengasamy, R.A. Johns, Chronic hypoxia upregulates endothelial and inducible NO synthase gene and protein expression in rat lung, Am. J. Physiol. 270 (1996) L164–L170.
[11] C. Iadecola, X. Xu, F. Zhang, E.E. El-Fakahany, M.E. Ross, Marked induction of calcium-independent nitric oxide synthase activity after focal cerebral ischemia, J. Cereb. Blood Flow Metab. 15 (1995) 52–59.
[12] R.S. Clark, P.M. Kochanek, M.A. Schwarz, J.K. Schiding, D.S. Turner, M. Chen, T.M. Carlos, S.C. Watkins, Inducible nitric oxide synthase expression in cerebrovascular smooth muscle and neutrophils after traumatic brain injury in immature rats, Pediatr. Res. 39 (1996) 784–788.
[13] M.A. Moro, R.J. Russell, S. Celleck, I. Lizasoain, Y. Su, V.M. Darley-Usmar, M.W. Radomski, S. Moncada, cGMP mediates the vascular and platelet actions of nitric oxide: confirmation using an inhibitor of the soluble guanylyl cyclase, Proc. Natl. Acad. Sci. USA 93 (1996) 1480–1485.

[14] D.S. Bredt, Endogenous nitric oxide synthesis: biological functions and pathophysiology, Free Radic. Res. 31 (1999) 577–596.
[15] B.E. Robertson, R. Schubert, J. Heschler, M.T. Nelson, cGMP-dependent protein kinase activates Ca^{2+}-activated K^+ channels in cerebral artery smooth muscle cells, Am. J. Physiol. 265 (1993) C299–C303.
[16] H. Taguchi, D.D. Heisted, Y. Chu, C.D. Rios, H. Ooboshi, F.M. Faraci, Vascular inducible nitric oxide synthase is associated with activation of Ca^{2+}-dependent K^+ channels, J. Pharmacol. Exp. Ther. 279 (1996) 1514–1519.
[17] J. Taniguchi, K.-I. Furukawa, M. Shigekawa, Maxi K^+ channels are stimulated by cyclic guanosine monophosphate-dependent protein kinase in canine coronary artery smooth muscle cells, Pflügers Arch. 423 (1993) 167–172.
[18] H. Miyoshi, Y. Nakaya, Endotoxin-induced nonendothelial nitric oxide activates the Ca^{2+}-activated K^+ channel in cultured vascular smooth muscle cells, J. Mol. Cell. Cardiol. 26 (1994) 1487–1495.
[19] S. Hall, S. Turcato, L. Clapp, Abnormal activation of K^+ channels underlies relaxation to bacterial lipopolysaccharide in rat aorta, Biochem. Biophys. Res. Commun. 224 (1996) 184–190.
[20] S.J. Chen, C.C. Wu, M.H. Yen, Role of nitric oxide and K^+ channels in vascular hyporeactivity induced by endotoxin, Nauyn-Schmiedebergs Arch. Pharmacol. 359 (1999) 493–499.
[21] C. Mertineit, L. Samlasingh-Parker, M. Glibetic, G. Ricard, F.J.D. Noya, J.V. Aranda, Nitric oxide, prostaglandins, and impaired cerebral blood flow autoregulation in group B streptococcal neonatal meningitis, Can. J. Physiol. Pharmacol. 78 (2000) 217–227.
[22] K.Y. Chyu, P. Dimayuga, J. Zhu, J. Nilsson, S. Kaul, P.K. Shah, B. Cercek, Decreased neointimal thickening after arterial wall injury in inducible nitric oxide synthase knockout mice, Circ. Res. 85 (1999) 1192–1198.
[23] C.C. Gunnett, Y. Chu, D.D. Heistad, A. Loihl, F.M. Faraci, Vascular effects of LPS in mice deficient in expression of the gene for inducible nitric oxide synthase, Am. J. Physiol. 275 (1998) H416–H421.
[24] J.D. MacMicking, C. Nathan, G. Horn, N. Chartrain, D.S. Fletcher, M. Trumbauer, K. Stevens, Q.W. Xie, K. Sokol, N. Hutchinson, H. Chen, J.S. Mudgett, Altered responses to bacterial infection and endotoxic shock in mice lacking inducible nitric oxide synthase, Cell 81 (1995) 641–650.
[25] S.C. Nicholson, R.T. Hahn, S.R. Grobmeyer, J.E. Brause, A. Hafner, S. Potter, R.B. Devereux, C.F. Nathan, Echocardiographic and survival studies in mice undergoing endotoxic shock: effects of genetic ablation of inducible nitric oxide synthase and pharmacologic antagonism of platelet-activating factor, J. Surg. Res. 86 (1999) 198–205.
[26] L. Hoang, D.A. Mathers, Bacterial endotoxin alters the kinetics of BK channels in rat cerebrovascular smooth muscle cells, Biochim. Biophys. Acta 1369 (1998) 335–345.
[27] L. Hoang, D.A. Mathers, Internally applied endotoxin and the activation of BK channels in cerebral artery smooth muscle via a nitric oxide-like pathway, Br. J. Pharmacol. 123 (1998) 5–12.
[28] M.J. Alonso, M.A. Rodriguez-Martinez, J. Martinez-Orgado, J. Marin, M. Salaices, The L-arginine inhibition of rat middle cerebral artery contractile response is mediated by inducible nitric oxide synthase, J. Auton. Pharmacol. 18 (1998) 105–113.
[29] F.T. Horrigan, J. Cui, R.W. Aldrich, Allosteric voltage gating of potassium channels I. Mslo ionic currents in the absence of Ca^{2+}, J. Gen. Physiol. 114 (1999) 277–304.
[30] F.T. Horrigan, R.W. Aldrich, Allosteric voltage gating of potassium channels II. Mslo channel gating charge movement in the absence of $Ca^{(2+)}$, J. Gen. Physiol. 114 (1999) 305–336.
[31] R. Brenner, G.J. Perez, A.D. Bonev, D.M. Eckman, J.C. Ckosek, S.W. Wiler, A.J. Patterson, M.T. Nelson, R.W. Aldrich, Vasoregulation by the β1 subunit of the calcium-activated potassium channel, Nature 407 (2000) 870–876.
[32] Y. Wang, D.A. Mathers, Ca^{2+}-dependent K^+ channels of high conductance in smooth muscle cells isolated from rat cerebral arteries, J. Physiol. 462 (1993) 529–545.
[33] B. Palacios, X. Cheng, C.C. Pang, Reversal of the in vitro lipopolysaccharide-induced suppression of contraction in rat aorta by N^G-nitro-arginine, diphenyleneiodonium and di-2-thienyliodonium, Eur. J. Pharmacol. 296 (1996) 75–79.
[34] R. Wang, L. Wu, The chemical modification of KCa channels by carbon monoxide in vascular smooth muscle cells, J. Biol. Chem. 272 (1997) 8222–8226.
[35] E. Morales, W.C. Cole, C.V. Remillard, N. Leblanc, Block of large conductance Ca^{2+}-activated K^+ channels in rabbit vascular myocytes by internal Mg^{2+} and Na^+, J. Physiol. 495 (1996) 701–716.
[36] V.A. Snetkov, A.M. Gurney, J.P. Ward, O.N. Osipenko, Inward rectification of the large conductance potassium channel in smooth muscle cells from rabbit pulmonary artery, Exp. Physiol. 81 (1996) 743–753.
[37] A.M. Briones, M.J. Alonso, J. Marin, M. Salaices, Role of iNOS in the vasodilator responses induced by L-arginine in the middle cerebral artery from normotensive and hypertensive rats, Br. J. Pharmacol. 126 (1999) 111–120.
[38] D.D. Rees, S. Cellek, R.M.J. Palmer, S. Moncada, Dexamethasone prevents the induction by endotoxin of a nitric oxide synthase and the associated effects on vascular tone: an insight into endotoxin shock, Biochem. Biophys. Res. Commun. 173 (1990) 541–547.
[39] E. Senba, T. Ueyama, Stress-induced expression of immediate early genes in the brain and peripheral organs of the rat, Neurosci. Res. 29 (1997) 183–207.
[40] G. Melillo, T. Musso, A. Sica, L.S. Taylor, G.W. Cox, L. Varesio, A hypoxia-responsive element mediates a novel pathway of activation of the inducible nitric oxide synthase promoter, J. Exp. Med. 182 (1995) 1683–1693.
[41] Y. Vodowotz, D. Russell, Q.W. Xie, C. Bogdan, C. Nathan, Vesicle membrane association of nitric oxide synthase in primary mouse macrophages, J. Immunol. 154 (1995) 2914–2925.

[42] T. Ishiwata, F. Guo, Z. Naito, G. Asano, R. Nishigaki, Differential distribution of ecNOS and iNOS mRNA in rat heart after endotoxin administration, Jpn. Heart J. 38 (1997) 445–455.
[43] R. Laporte, I. Laher, Sarcoplasmic reticulum–sarcolemma interactions and vascular smooth muscle tone, J. Vascular Res. 34 (1997) 325–343.
[44] A. Wei, C. Solaro, C. Lingle, L. Salkoff, Calcium sensitivity of BK-type KCa channels determined by a separable domain, Neuron 13 (1994) 671–681.
[45] M. Wallner, P. Meera, L. Liga, Determinants for β-subunit regulation in high-conductance voltage-activated and Ca^{2+}-sensitive K^+ channels: An additional transmembrane region at the N terminus, Proc. Natl. Acad. Sci. USA 93 (1996) 14922–14927.
[46] S.S. Segal, S.E. Brett, W.C. Sessa, Codistribution of NOS and caveolin throughout peripheral vasculature and skeletal muscle of hamsters, Am. J. Physiol. 277 (1999) H1167–H1177.
[47] T.S. Sherman, Z. Chen, I.S. Yuhanna, K.S. Lau, L.R. Margraf, P.W. Shaul, Nitric oxide synthase isoform expression in the developing lung epithelium, Am. J. Physiol. 276 (1999) L383–L390.
[48] C.M. Brophy, L. Knoepp, J. Xin, J.S. Pollock, Functional expression of NOS 1 in vascular smooth muscle, Am. J. Physiol. 278 (2000) H991–H997.
[49] P.M. Schwarz, H. Kleinert, U. Forstermann, Potential functional significance of brain-type and muscle-type nitric oxide synthase I expressed in adventitia and media of rats, Arterioscler. Thromb. Vasc. Biol. 19 (1999) 2584–2590.
[50] M. Trovati, P. Massucco, L. Mattiello, C. Costamagna, E. Aldieri, F. Cavalot, G. Anfossi, A. Bosia, D. Ghigo, Human vascular smooth muscle cells express a constitutive nitric oxide synthase that insulin rapidly activates, thus increasing guanosine 3′:5′-cyclic monophosphate and adenosine 3′:5′-cyclic monophosphate concentrations, Diabetologia 42 (1999) 831–839.
[51] J.E. Brenman, D.S. Chao, S.H. Gee, A.W. McGee, S.E. Craven, D.R. Santillano, Z. Wu, F. Huang, H. Xia, M.F. Peters, S.C. Froehner, D.S. Bredt, Interaction of nitric oxide synthase with the postsynaptic density protein PSD-95 and alpha1-syntrophin mediated by PDZ domains, Cell 84 (1996) 757–767.
[52] R. Das, G.M. Kravtsov, H.J. Ballard, C.Y. Kwan, L-NAME inhibits Mg^{2+}-induced rat aortic relaxation in the absence of endothelium, Br. J. Pharmacol. 128 (1999) 493–499.